Fish and Shellfish Immunology 95 (2019) 171–179

Contents lists available at ScienceDirect

Fish and Shellfish Immunology

journal homepage: www.elsevier.com/locate/fsi

Full length article

The L-domains in M and G proteins of infectious hematopoietic necrosis virus (IHNV) affect viral budding and pathogenicity

Yaping Chen, Jiahui Li, Dechuan Li, Xin Guan, Xuanyu Ren, Ying Zhou, Ying Feng, Shuai Gao, Na Wang, Xueting Guan, Wen Shi, Min Liu*

College of Animal Science and Technology, Northeast Agricultural University, Harbin, 150030, People's Republic of China

ARTICLE INFO

Keywords:
Infectious hematopoietic necrosis virus
Late-domain
Budding
Pathogenicity

ABSTRACT

RNA viruses including many retroviruses encode "late-domain" motifs that can interact with host proteins to mediate viral assembly and affect viral budding and pathogenicity. For IHNV, our previous studies demonstrated that the respective interactions of the L domains of IHNV with host proteins could mediate viral assembly and budding. To our knowledge, the role of L domains of the IHNV in the budding and pathogenicity has not investigated yet. In this study, we generated two recombinant IHNV strains rIHNV-$M_{(PH > A4)}$ and rIHNV-$G_{(PS > A4)}$ with mutations in the L domains (PPPH to AAAA or PSAP to AARA) of IHNV by reverse genetics and explored the effect of the mutations on budding and pathogenicity of the two recombinant viruses. The RT-qPCR results showed that the production levels of the extracellular particles of rIHNV-$M_{(PH > A4)}$ or rIHNV-$G_{(PS > A4)}$ declined significantly, compared with those of wild-type (wt) IHNV HLJ-09. Furthermore, the challenge test showed that the survival rates of juvenile rainbow trout challenged with rIHNV-$M_{(PH > A4)}$ or rIHNV-$G_{(PS > A4)}$ were 90% or 87%, respectively; however, the survivability was zero in groups challenged with wtIHNV HLJ-09 or rIHNV HLJ-09 (recombinant IHNV). Additionally, the RT-qPCR results showed that the recombinant viruses induced higher expression levels of *IFN1, IL-1β,* and *IL-8* compared with those induced by wtIHNV HLJ-09 as well as the ELISA results showed that fish vaccinated with recombinant viruses produced high levels of specific IgM antibodies, demonstrating that the two recombinant viruses may induce immune responses to resist infection by IHNV. Also, these results demonstrated for the first time that the L domains of the M and G proteins of IHNV could affect the budding and pathogenicity of IHNV, which may be beneficial in the prevention and control of IHNV infections in fish. Taken together, our study as the first research provides the foundation for effect of rhabdovirus L domains on viral budding and pathogenicity.

1. Introduction

Infectious hematopoietic necrosis virus (IHNV) is the causative agent of infectious hematopoietic necrosis (IHN) [1], which is characterized by hemorrhage and necrosis of hematopoietic tissue and other internal organs. First described in western North America in the early 1950s, IHN is now widespread across the Pacific coast of Canada and the United States, Europe, Asia, and Iran [2–6]. IHNV is a member of the *Novirhabdovirus* genus in the *Rhabdoviridae* family of viruses [4]. Outbreaks of IHNV infection are well known to cause mass mortality worldwide in the salmonid fish [5–9]. IHNV has a negative-sense, single-stranded RNA genome of approximately 11 kilobases (kb), which encodes six proteins that include nucleoprotein (N), polymerase-associated phosphoprotein (P), matrix protein (M), unique glycoprotein (G), sizeable RNA-dependent RNA polymerase (L) [10–14] and a short gene located between the G and L genes that encodes a nonstructural protein (NV) [15–18]. The M protein is a multifunctional protein involved not only in viral assembly and budding but also in viral pathogenicity [19]. Moreover, the carboxy terminus of the viral glycoprotein is embedded in the membrane matrix protein dimer and binds to the glycoprotein through hydrophobic and electrostatic interactions, which contributes to the formation of the viral glycoprotein trimer and promotes the assembly and budding of the virus [20,21].

Most of the enveloped viruses have late-budding domains (L-domains) [22], which facilitate viral budding by interacting with usurping specific host proteins or machinery, most of which are components of the vacuolar protein sorting (VPS) or endosomal sorting complex required for transport (ESCRT) pathways during late stages of viral

* Corresponding author. College of Animal Science and Technology, Northeast Agricultural University, Chang Jiang Road No. 600, Xiang Fang District, Harbin, People's Republic of China. Tel.: 86 045155191385.
E-mail address: liumin-707@163.com (M. Liu).

https://doi.org/10.1016/j.fsi.2019.10.030
Received 31 July 2019; Received in revised form 7 October 2019; Accepted 11 October 2019
Available online 11 October 2019

replication [23,24]. There are now three distinct L domains that have been identified and associated with budding defects within the retrovirus family, with core amino acid motifs PT/SAP, PPXY, or YPXL/LXXLF [25–27]. Two of the best-characterized L-domains core motifs are PPPY and PT/SAP [28]. The PPPY motif is known to interact with WW domain-containing ubiquitin ligases, such as Nedd4, and other members of the HECT family of E3 ubiquitin ligases [29,30]. Additionally, the PPPY motif of vesicular stomatitis virus (VSV) is critical for efficient budding and interactions with host proteins in the context of VSV infection [30]. The PT/SAP motif is known to directly interact with tsg101, a component of ESCRT-I, and is involved in the MVB sorting pathway in mammalian cells [30,31]. Moreover, previous studies have shown that mutations in the PSAP region of the matrix protein of VSV lead to the attenuation of VSV [19]. For IHNV M protein, the L-domain motif is composed of a PPPH core located at amino acids 14–17 of the M protein. The L-domain motif in the M protein of IHNV directly interacts with Nedd4. Also, the L-domain motif is composed of a PSAP core located at amino acids 493–496 of the G protein, which interacts with Tsg101. The respective interactions of the L domains of IHNV with host proteins could mediate viral assembly and budding [32]. However, the ability of the PPPH and PSAP motifs within the IHNV M and G proteins to function as bona fide L-domains for IHNV budding and pathogenicity remains to be determined.

In this study, two recombinant IHNV mutants, rIHNV-$M_{(PH > A4)}$ and rIHNV-$G_{(PS > A4)}$, with mutations of the PPPH residues of the M protein and the PSAP residues of the G protein were generated by reverse genetics to determine whether L-domains are indeed critical for viral budding. Moreover, we evaluated the immunomodulatory effect of the two recombinant IHNV mutants on rainbow trout. The results illustrate the importance of the L-domains in the M and G proteins of IHNV on viral budding and pathogenicity, providing a better understanding of IHNV budding and aiding the development of more effective strategies for the prevention and control of IHNV infections. Additionally, they may provide beneficial insight into the viral pathogenesis of IHNV.

2. Materials and methods

All applicable international and national guidelines for the care and use of animals were followed. The animal experiments were approved by the Institutional Committee of Northeast Agricultural University.

2.1. Cells, plasmids, viruses, and antibodies

Chinook salmon embryo (CHSE-214) cells, Epithelioma papulosum cyprinid (EPC) cells, and rainbow trout gonad (RTG-2) cells were obtained from the American Type Culture Collection (Manassas, VA, USA) and grown in L15 (Leibovitz) medium supplemented with 10% fetal bovine serum (FBS). The full-length genome plasmids pBlueScript II-IHNV HLJ-09, pCI-N, pCI-P, pCI-NV, pCI-G, pCI-L, pT-F2, and pT-F3 were designed in our laboratory [33]. The wild-type (wt) IHNV HLJ-09 viral strain (accession number JX649101) was isolated at our laboratory, and the recombinant IHNV (rIHNV HLJ-09) was generated by reverse genetics in our laboratory and used in this study [33]. Rabbit anti-rainbow trout IgM serum antibody and mouse anti-IHNV antibodies were prepared previously in our laboratory as previously described [33]. Fluorescein isothiocyanate (FITC)-conjugated goat anti-mouse IgG, horseradish peroxidase (HRP)-conjugated goat anti-mouse IgG antibodies, and horseradish peroxidase (HRP)-conjugated goat anti-rabbit IgG antibodies were purchased from Thermo Fisher Scientific (Waltham, MA) [18].

2.2. Plasmid construction

In this order, HamF1, F2, F3, F4, F5, and HdvF6 were gene fragments sequentially cloned into *NheI/SnaBI, SnaBI/NdeI, NdeI/SpeI, SpeI/MluI, MluI/NcoI,* and *NcoI/KpnI* positions on the MCS of the pBlueScript II SK (+). The correct recombinant plasmid was named pBlueScript II-IHNV HLJ-09. We mutated proline-proline-proline-histidine (PPPH) to alanine-alanine-alanine-alanine (AAAA) at positions 14–17 of the M protein using PCR to amplify the gene with the primers IHNV SnaBF*/IHNV $M_{(PH > A4)\ R}$ and IHNV $M_{(PH > A4)\ F}$/IHNV $M_{(PH > A4)}$ NdeR on the pT-F2, respectively. The purified PCR products were used for overlapping extension PCR by using the primers IHNV SnaBF*/IHNV $M_{(PH > A4)}$ NdeR (pMD18-T-F2-$M_{(PH > A4)}$). Additionally, we mutated proline-serine-alanine-proline (PSAP) to alanine-alanine-arginine-alanine (AARA) at positions 493–496 of the G protein using PCR to amplify genes using the primers IHNV $G_{(PS > A4)}$ NdeF/IHNV $G_{(PS > A4)\ R}$ and IHNV $G_{(PS > A4)\ F}$/IHNV SpeR* on the pT-F3, respectively. The purified PCR products were used for overlapping extension PCR with the primers IHNV $G_{(PS > A4)}$ NdeF/IHNV SpeR* (pMD18-T-F3-$G_{(PS > A4)}$). Next, pMD18-T-F2-$M_{(PH > A4)}$ or pMD18-T-F3-$G_{(PS > A4)}$ was purified and inserted into the restriction enzyme cutting sites *SnaBI/NdeI or NdeI/SpeI* of pBlueScript II-IHNV HLJ-09, respectively. The correct recombinant plasmids were named pBlueScript II-IHNV-$M_{(PH > A4)}$ and pBlueScript II-IHNV-$G_{(PS > A4)}$. The pBlueScript II-IHNV-$M_{(PH > A4)}$ and pBlueScript II-IHNV-$G_{(PS > A4)}$ constructs were digested with *NheI* and *KpnI* and subcloned into the pCI plasmid, which was predigested with the same restriction enzymes. The final constructs were named pCI-$M_{(PH > A4)}$ and pCI-$G_{(PS > A4)}$, respectively. The cloning strategy is shown in Fig. 1. The primers used are shown in Table 1. The purified PCR products were sequenced by Comate Bioscience Company Limited (Jilin, China).

2.3. Recovery of two recombinant viruses

Recovery of recombinant viruses was carried out as previously described [33]. Briefly, the pCI-$M_{(PH > A4)}$ (0.5 μg) or pCI-$G_{(PS > A4)}$ (0.5 μg) plasmid in combination with the pCI-N (0.25 μg), pCI-P (0.25 μg), pCI-L (0.1 μg), pCI-NV (0.05 μg), and pCI-G (0.05 μg) plasmids were cotransfected into CHSE-214 cells using Lipofectamine LTX & Plus Reagent (Invitrogen, Life Technologies, Carlsbad, CA, USA) at 22 °C. The transfected cells were washed and maintained in L15 medium containing 10% FBS at 15 °C for 5–7 days. The cell monolayer was observed for the development of virus-induced cytopathic effect (CPE), and then the supernatant was harvested and clarified for further processing of the recombinant viruses.

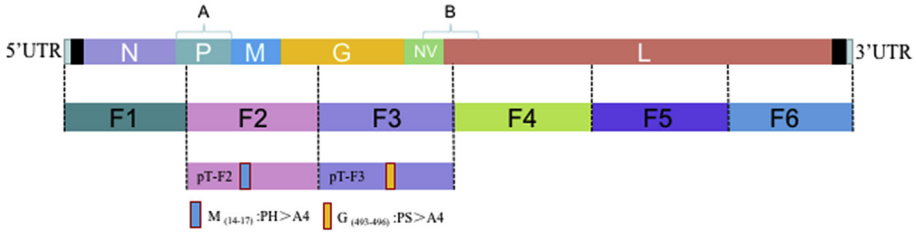

Fig. 1. Construction strategy of recombinant viruses. Coding regions (ORFs) of M, in which the nucleotides encoding ^{14}PPPH^{17} were mutated into ^{14}AAAA^{17} from the M of pT-F2, were amplified using fusion PCR. Coding regions (ORFs) of G, in which the nucleotides encoding ^{493}PSAP^{496} were mutated into ^{493}AARA^{496} from the G of pT-F3, were amplified using fusion PCR.

Table 1
Summary of sequences used in this study. Italics and bold portion indicate enzyme sites for genetic tags. Asterisks show that the nucleotides were silent mutations. Underlined portion indicates point mutant sites. All primers used in this study were designed using Primer Premier 5.0.

Primer names	Primer sequences (5′-3′)	Targets (ID)
Primers for the construction of plasmids for recombinant viruses and identification of recombinant viruses by genetic tags		
IHNV SnaBF*	CTAAAA***TACGTA***GAGGAGGAG	JX649101
IHNV $M_{(PH > A4)\ R}$	GGCAGCAGCAGCGATCAGAACTGTTCTCTTTGCTCTCTTGAAAATGGACAT	JX649101
IHNV $M_{(PH > A4)\ F}$	ATGTCCATTTTCAAGAGAGCAAAGAGAACAGTTCTGATCGCTGCTGCTGCC	JX649101
IHNV $M_{(PH > A4)}$ NdeR	TGTGGTGT***CATATG***CCCCTGC	JX649101
IHNV $G_{(PS > A4)}$ NdeF	GCAGGGG***CATATG***ACACCACA	JX649101
IHNV $G_{(PS > A4)\ R}$	GGACCTGTTTGCCAGGTGATACATGGGGATACTCTGAGCCCGAGCAGC	JX649101
IHNV $G_{(PS > A4)\ F}$	GCTGCTCGGGCTCAGAGTATCCCCATGTATCACCTGGCAAACAGGTCC	JX649101
IHNV SpeR*	TGCATGGAG***ACTAGT***GGAGTCGTTG	JX649101
IHNV P KpnF	***GGTACC***GCCACCATGTCAGATGGAGA	JX649101
IHNV P NotR rIHN SpeF	***GCGGCCGC***CTATTGACCCTGCTTCA T	JX649101
rIHN SpeR	CGAGTATTGTACATGGACCTCAGCA	JX649101
	GGACTACCCCCTCCACGAACTCT	JX649101
Primers used in the quantitative real-time PCR		
qIFN1-F	GCGAAACAAACTGCTATTTACAATGTATA	IFN1
qIFN1-R	TCACAGCAATGACACACACGCTC	(AJ580911.2)
qIL-8-F	ACCATTACTGAGGGGATGAGTCTGA	IL-8
qIL-8-R	CATCTCCACCTTCTTAATGAGCCTA	(DQ778949)
qIL-1βF	GGAGAGGTTAAAGGGTGGCGA	IL-1β
qIL-1βR	TGCCGACTCCAACTCCAACA	(AJ278242.2)
qTNF-αF	AGCATGGAAGACCGTCAACGAT	TNF-α
qTNF-αR	ACCCTCTAAATGGATGGCTGCTT	(NM001124357.1)
qEF-1α-F	CAAGGATATCCGTCGTGGCA	EF-1α
qEF-1α-R	ACAGCGAAACGACCAAGAGG	(AF498320)
Primers for identification of IHNV by real-time PCR		
IHNV-F	AGAGTTCGTGGAGGGGGTAGTC	JX649101
IHNV-R	GGCAAGGAAGTCCGCATACG	JX649101

2.4. Identification of recombinant viruses

2.4.1. Reverse transcription PCR (RT-PCR) and identification of recombinant viruses using genetic tags

The viral genomic RNA was extracted from the fifth cell culture passage of the recombinant viruses and wtIHNV HLJ-09 and was used to confirm the sequence of the mutated regions of the L domain by PCR using IHNV SnaBF*/IHNV $M_{(PH > A4)}$ NdeR or IHNV $G_{(PS > A4)}$ NdeF/IHNV SpeR*. The purified PCR products were sequenced by Comate Bioscience Company Limited. We confirmed the presence of genetic tags artificially introduced by RT-PCR. Fragment A of wtIHNV HLJ-09, rIHNV-$M_{(PH > A4)}$ and rIHNV-$G_{(PS > A4)}$ was amplified by PCR using the primers IHNV P KpnF and IHNV P NotR and digested by endonuclease *SnaBI*. Fragment B of the viruses was amplified by PCR using the primers rIHN SpeF and rIHN SpeR (Table 1). The PCR products were purified and digested with endonuclease *SpeI*. The RT-PCR products were also sequenced to confirm the introduction of the *SnaBI* and *SpeI* restriction sites [33–35].

2.4.2. Indirect immunofluorescence assay

CHSE-214 cells infected with rIHNV-$M_{(PH > A4)}$ or rIHNV-$G_{(PS > A4)}$ in 24-well plates were cultured for 60 h at 15 °C. Uninfected cells and cells infected with wtIHNV HLJ-09 were used as negative and positive controls, respectively. IFA was performed as described previously, and the immunoblots were developed using mouse anti-IHNV as the primary antibody and followed by incubation with fluorescein isothiocyanate (FITC)-conjugated goat anti-mouse IgG [34].

2.4.3. Identification of recombinant viruses using transmission electron microscopy (TEM)

After 60 h of inoculation with the appropriate rIHNV-$M_{(PH > A4)}$ or rIHNV-$G_{(PS > A4)}$ constructs, the CHSE-214 cells were scraped off, fixed with 2% glutaraldehyde at 4 °C for 2 h, washed with PBS, fixed, dehydrated, embedded, and polymerized. The embedded samples were sectioned using an ultramicrotome. Then, the sections were stained with uranyl acetate and lead citrate and the morphology of the virus particles was observed by TEM [35].

2.5. Determination of recombinant IHNV growth curves and cell tropism

The titers of rIHNV-$M_{(PH > A4)}$, rIHNV-$G_{(PS > A4)}$, rIHNV HLJ-09 and wtIHNV HLJ-09 improved with increasing serial passages in CHSE-214 cells. CHSE-214 cells in 96-well plates were incubated with 100 µl of viral samples at 15 °C for five days. The cytopathic effect (CPE) was observed, and the viral titers ($TCID_{50}$/mL) were calculated by the Reed-Muench method [18,36]. The cells were infected with rIHNV-$M_{(PH > A4)}$, rIHNV-$G_{(PS > A4)}$, rIHNV HLJ-09 or wtIHNV HLJ-09 at 100 $TCID_{50}$, and the supernatants were sampled at 12, 24, 36, 48, 60, 72, 84, and 96 h. The titers ($TCID_{50}$/mL) of these samples were calculated according to the above methods, and the corresponding growth curves were generated [18]. To evaluate the cell tropisms of rIHNV-$M_{(PH > A4)}$ and rIHNV-$G_{(PS > A4)}$, EPC, CHSE-214, and RTG-2 cell monolayers were infected with 100 $TCID_{50}$ of wtIHNV HLJ-09, rIHNV HLJ-09 or the two recombinant IHNV strains. The cells were cultured at 16 °C for 72 h and viral titers (log10 $TCID_{50}$/mL) were calculated by the Reed-Muench method [36,37].

2.6. Determination of the levels of IHNV GE of recombinant viruses

Cells cultured in 6-well plates were infected with rIHNV-$M_{(PH > A4)}$, rIHNV-$G_{(PS > A4)}$, rIHNV HLJ-09 or wtIHNV HLJ-09 at 100 $TCID_{50}$, and the supernatants and CHSE-214 cells were sampled at 72 h. Then, 250 µl of the samples was used for the extraction of total RNA by using an RNA extraction kit (Fastagen, China). The RNA concentration was measured by absorbance of the RNA sample, and the ratio of OD260/OD280 was between 1.9 and 2.1. Additionally, the RNA quality was analyzed based on the intensity of the band using agarose gel electrophoresis. Then, complementary DNA (cDNA) was generated via reverse transcription, which was used for absolute real-time qPCR (primer sequences in Table 1, accession number JX649101). Levels of IHNV GE were determined using Light Cycler 480 (Roche, CH). qPCR was carried out in triplicate per sample [32].

2.7. Pathogenicity of recombinant viruses

2.7.1. Pathogenicity test and protective efficacy of recombinant viruses

To assess the pathogenicity of the recombinant viruses, the viruses were used to infect healthy juvenile rainbow trout. The juvenile rainbow trout (mean weight ~ 2 g) were randomly allocated into five groups, with each group comprising 30 fish. The fish were injected with 50 μl (1×10^5 $TCID_{50}$/ml) of rIHNV-$M_{(PH > A4)}$, rIHNV-$G_{(PS > A4)}$, rIHNV HLJ-09 or wtIHNV HLJ-09 by intraperitoneal injection. Control fish were injected with the same volume of PBS. After immunization, juvenile rainbow trout were reared at 15 °C. Deaths were observed for 20 consecutive days. To further evaluate the protective efficacy of the recombinant viruses, juvenile rainbow trout were intraperitoneally injected with 50 μl (1×10^5 $TCID_{50}$/mL) of rIHNV-$M_{(PH > A4)}$ or rIHNV-$G_{(PS > A4)}$ and observed for 20 consecutive days. Then, the vaccinated rIHNV-$M_{(PH > A4)}$, rIHNV-$G_{(PS > A4)}$ and control groups (injected with the same volume of PBS) were divided into three groups and challenged with 50 μl (1×10^5 $TCID_{50}$/ml) of wtIHNV HLJ-09. Finally, the cumulative mortality was calculated, and it was obtained after 20 days [18]. The data were analyzed using the GraphPad Prism v 5.0 software.

2.7.2. Measurement of the recombinant viruses in vivo growth

The active replication of recombinant viruses in rainbow trout was detected using a SYBR Green-based quantitative real-time RT-PCR (RT-qPCR) assay. In brief, rainbow trout of mean weight 6 g were randomly assorted into 5 groups of ten fish each, which were injected with 200 μl (10^5 $TCID_{50}$/mL) of rIHNV-$M_{(PH > A4)}$, rIHNV-$G_{(PS > A4)}$, rIHNV HLJ-09, wtIHNV HLJ-09, or cell culture medium (L15) as a mock-infection negative control. After 72 h, viral genome copy numbers in fish liver and kidney samples were quantified by RT-qPCR using the IHNV F and IHNV R primers (primer sequences in Table 1, accession number JX649101). To calculate viral genome copy numbers, the plasmid pBlueScript II SK-F543216 containing the full-length cDNA of IHNV was used as a standard to establish the standard curve for the RT-qPCR assay [37]. The standard curve formula was $Y = -2.869X + 36.296$, $R^2 = 0.988$.

2.8. Host gene expression

To observe whether the transcriptional level of immune-related genes changed after inoculation with rIHNV-$M_{(PH > A4)}$ or rIHNV-$G_{(PS > A4)}$ in rainbow trout, the fish (mean weight = 6 g) were randomly divided into 5 groups, with each group comprising 20 fish. The fish were intraperitoneally injected with 200 μl (10^5 $TCID_{50}$/mL) of rIHNV-$M_{(PH > A4)}$, rIHNV-$G_{(PS > A4)}$, rIHNV HLJ-09 or wtIHNV HLJ-09. The control group was challenged with the same dose of cell culture medium. Fish were reared at 15 °C with a closed-circuit water system. The spleen tissues were sampled after infection for 24 h and 48 h, and 1 ml of sterile PBS was added to homogenize the mixture. A total of 250 μl of the samples was used for the extraction of total RNA by using an RNA extraction kit (Fastagen, China). Total RNA was reverse transcribed into cDNA, which was used as a fluorescent quantitative PCR template. The expression of *IFN1, IL-8, IL-1β, TNF-α,* and the reference gene *EF-1α* in tissues was detected by real-time fluorescence quantitative PCR. The primer sequences used in the fluorescent quantitative PCR are shown in Table 1, and the relative mRNA levels of *IFN1, IL-8, IL-1β,* and *TNF-α* were calculated according to the $2^{-\Delta\Delta Ct}$ method. We performed real-time PCR in triplicate [38].

2.9. Determination of the specific antibody IgM in the serum of rainbow trout

The rainbow trout (mean weight = 10 g) were intraperitoneally injected with 200 μl of rIHNV-$M_{(PH > A4)}$, rIHNV-$G_{(PS > A4)}$, rIHNV HLJ-09 or wtIHNV HLJ-09 (1×10^5 $TCID_{50}$/ml). Blood samples from these rainbow trout were collected after inoculation of 14, 28, 42, and 56 days. Blood samples from rainbow trout injected with the same volume of PBS were used as a control. The specific antibody IgM in the serum of rainbow trout was detected using indirect ELISA [34]. Briefly, 100 μl of wtIHNV HLJ-09 was coated in each well of a 96-well ELISA plate overnight at 4 °C, followed by serial two-fold dilutions of pooled sera from each group of rainbow trout. Samples were then incubated with rabbit anti-rainbow trout IgM serum antibody (1:1000). Next, 100 μl of HRP-labeled goat anti-rabbit IgG (1:2000) was added. Finally, a *t*-test was conducted to test whether there was a significant difference in the antibody IgM levels between these groups [18].

2.10. Statistical analysis

All experiments were performed at least three times with reproducible results. Student's t-test was used to determine statistical significance. P-values less than 0.05 were considered statistically significant, and those less than 0.01 were considered highly significant.

3. Results

3.1. Identification of the two recombinant viruses

After transfection with pCI-$M_{(PH > A4)}$ or pCI-$G_{(PS > A4)}$, 80% of CHSE-214 cells displayed CPE by 7 days at 15 °C, whereas the control cells did not. To confirm that the recombinant viruses were derived from rIHNV-$M_{(PH > A4)}$ or rIHNV-$G_{(PS > A4)}$, sequencing chromatographs of the mutated regions of the L domains in the recombinant IHNV and the same region in wtIHNV HLJ-09 were compared as shown in Fig. 2A and B. The results showed that the L domains of the two recombinant viruses were mutated successfully. Fragment A (690 bp) and fragment B (740 bp) of rIHNV-$M_{(PH > A4)}$, rIHNV-$G_{(PS > A4)}$ or wtIHNV HLJ-09 were amplified by RT-PCR. For fragment A, the digested product sizes of the rescued viruses were approximately 220 bp and 470 bp, whereas the corresponding fragment of wtIHNV HLJ-09 could not be digested by *SnaBI* (Fig. 2C). Additionally, for fragment B, the digested product sizes of rescued viruses were approximately 290 bp and 450 bp, whereas the corresponding fragment of wtIHNV HLJ-09 could not be digested by *SpeI* (Fig. 2D). These results show that the recombinant viruses are indeed derived from the transfected eukaryotic expression plasmid. Moreover, to determine whether the recombinant viruses were rescued successfully, CHSE-214 cells infected with rIHNV-$M_{(PH > A4)}$, rIHNV-$G_{(PS > A4)}$ or wtIHNV HLJ-09 in 24-well plates were cultured for 60 h at 15 °C for immunofluorescence assay (Fig. 3). The results showed that specific green signals were observed in the rIHNV-$M_{(PH > A4)}$, rIHNV-$G_{(PS > A4)}$ and wtIHNV HLJ-09-infected CHSE-214 cells, but no specific green signal was detected in the mock-infected control cells. Then, CHSE-214 cells infected with rIHNV-$M_{(PH > A4)}$, rIHNV-$G_{(PS > A4)}$, and wtIHNV HLJ-09 showed typical bullet-shaped virions that were ~80 nm in diameter and up to 160 nm in length, which was similar to those of other Rhabdoviridae viruses (Fig. 3F and G).

3.2. Growth curves and cell tropisms of the recombinant viruses

To determine the growth curves of the recombinant viruses in CHSE-214 cells, the viral titers were determined at 12 h intervals post-infection. The results showed that the two recombinant viruses had similar copy features with wtIHNV HLJ-09. Their logarithmic phase occurred at 24–60 h post-infection, and the platform stage occurred at 72 h post-infection. The viral titers of rIHNV-$M_{(PH > A4)}$ and rIHNV-$G_{(PS > A4)}$ were 10^6 $TCID_{50}$/ml, which were lower than those of rIHNV HLJ-09 and wtIHNV HLJ-09, indicating that the mutations of the L-domains can affect the replication ability of the virus to some extent (Fig. 4A). Moreover, we found that the cell tropisms of the two recombinant viruses were comparable to those of wtIHNV HLJ-09, as determined by comparing viral titers in CHSE-214, EPC, and RTG-2 cells at 72 h post-infection (Fig. 4B). Additionally, the viral titers of

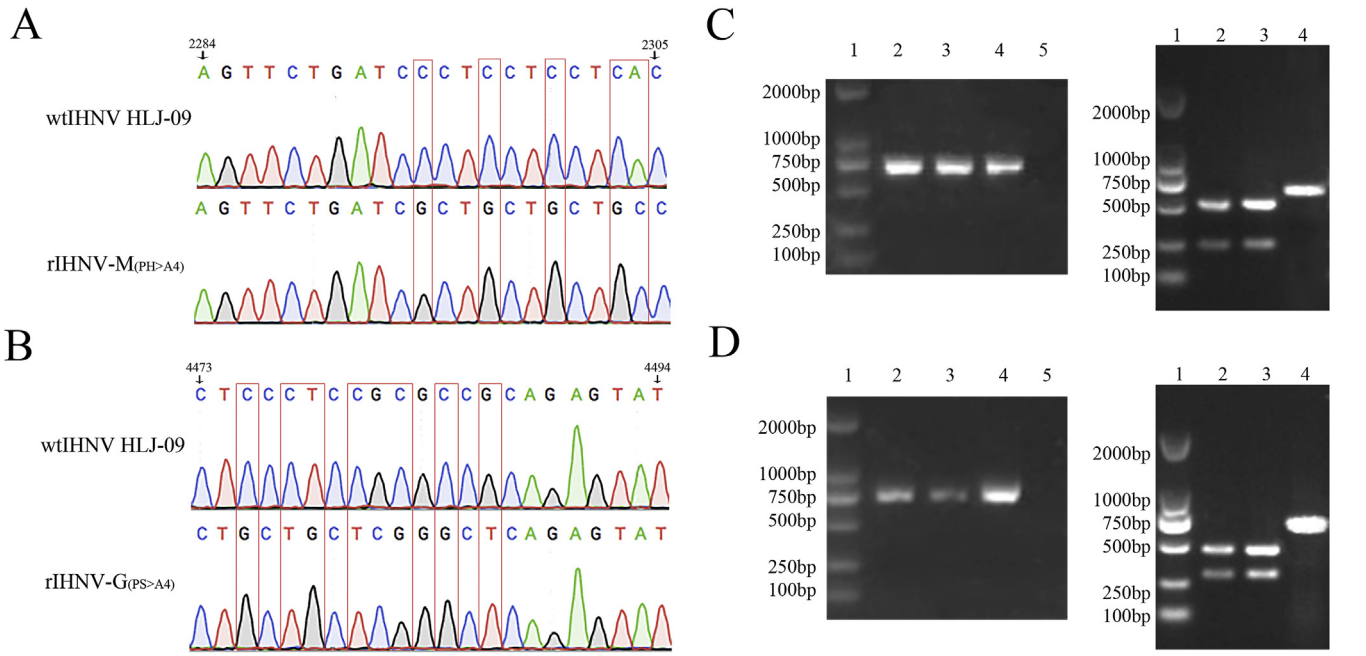

Fig. 2. Analysis of sequence and genetic tags for recombinant viruses. In A, the sequencing chromatographs of the mutation regions of L domain in rIHNV-$M_{(PH > A4)}$ and the same region in wtIHNV HLJ-09 was shown by red text box at 2294–2304 bp in the full-length IHNV. The same and mutation of the sequencing region of rIHNV-$G_{(PS > A4)}$ and wtIHNV HLJ-09 was shown in B. In C (left), genomic RNA isolated from the wtIHNV HLJ-09 and the recombinant viruses were amplified by RT-PCR with two specific primers covering the regions, rIHNV-$M_{(PH > A4)}$ (Line 2), rIHNV-$G_{(PS > A4)}$ (Line 3) and wtIHNV HL-09 (Line 4), negative control (Line 5). In C (right), digestion analyses of *SnaBI* were performed in rIHNV-$M_{(PH > A4)}$ (Line 2), rIHNV-$G_{(PS > A4)}$ (Line 3), wtIHNV HLJ-09 (Line 4), and analyzed on a 1% agarose gel. In D, line 2, 3 and 4 were fragment B amplified from rIHNV-$M_{(PH > A4)}$, rIHNV-$G_{(PS > A4)}$ and wtIHNV HLJ-09, respectively (left) and their corresponding products were digested by *SpeI* (right). (For interpretation of the references to colour in this figure legend, the reader is referred to the Web version of this article.)

the two recombinant viruses were significantly higher in the EPC and CHSE-214 cells compared with the RTG-2 cells.

3.3. Determination of the levels of IHNV GE of the recombinant viruses

To determine the production levels of the extracellular IHNV particles and the production of the corresponding intracellular IHNV GEs, CHSE-214 cells were infected with rIHNV-$M_{(PH > A4)}$, rIHNV-$G_{(PS > A4)}$, rIHNV HLJ-09 or wtIHNV HLJ-09 in 6-well plates. After 72 h, the levels of IHNV GE were determined by RT-qPCR. The results showed that the production levels of the extracellular IHNV particles from cells infected with rIHNV-$M_{(PH > A4)}$ or rIHNV-$G_{(PS > A4)}$ declined significantly compared with those in cells infected with rIHNV HLJ-09 and wtIHNV HLJ-09, although the production of the corresponding intracellular IHNV GEs was not affected (Fig. 5).

3.4. Pathogenicity of the recombinant viruses

Juvenile rainbow trout were infected with rIHNV-$M_{(PH > A4)}$, rIHNV-$G_{(PS > A4)}$, rIHNV HLJ-09, or wtIHNV HLJ-09, and then deaths were recorded for 20 consecutive days. The fish that were infected with wtIHNV HLJ-09 or rIHNV HLJ-09 began to die by day 4, and the peak of mortality was between days 6–8. By day 20, none of the fish infected with these viruses had survived, and all of them showed clinical symptoms associated with infection. However, the survival rates of fish infected with recombinant viruses rIHNV-$M_{(PH > A4)}$ or rIHNV-$G_{(PS > A4)}$ were 90% or 87%, respectively. This suggests that the recombinant viruses were highly attenuated (Fig. 6A). As shown in Fig. 6B, the survival rates of fish infected with the two recombinant viruses against wtIHNV HLJ-09 virus challenge were 80% and 75%, respectively. The survival rate of juvenile rainbow trout was much improved, demonstrating substantial immunoprotection conferred by rIHNV-$M_{(PH > A4)}$ and rIHNV-$G_{(PS > A4)}$ challenge. Moreover, we determined the genome copy numbers of recombinant viruses in the livers and kidneys of fish using RT-qPCR and found that in the fish infected with the recombinant viruses, the viral genome copy numbers in the liver (Fig. 6C) and kidney (Fig. 6D) were lower than those of fish infected with wtIHNV HLJ-09 and rIHNV HLJ-09, which was consistent with our earlier observations. These results suggested that the pathogenicity of the two recombinants in CHSE-214 cells was significantly lower than that of the wtIHNV HLJ-09.

3.5. The expression of cytokines in rainbow trout infected with the recombinant viruses

The spleen tissues of rainbow trout intraperitoneally infected with the recombinant viruses rIHNV-$M_{(PH > A4)}$, rIHNV-$G_{(PS > A4)}$, rIHNV HLJ-09 or wtIHNV HLJ-09 were sampled to detect the expression of *IFN1, IL-8, IL-1β,* and *T NF-α* cytokines at 24 h and 48 h pi. The results showed that the expression levels of *IFN1, IL-8* and *IL-1β* in the rIHNV-$M_{(PH > A4)}$ and rIHNV-$G_{(PS > A4)}$ groups increased relative to those in the rIHNV HLJ-09 and wtIHNV HLJ-09 groups ($P < 0.05$); however, there was no difference in the expression levels of *TNF-α*. The above experimental results show that the recombinant viruses rIHNV-$M_{(PH > A4)}$ and rIHNV-$G_{(PS > A4)}$ can induce the expression of interferon *IFN1*, proinflammatory cytokine *IL-1β* and chemokine *IL-8* (Fig. 7).

3.6. Identification of specific IgM antibodies in the serum of rainbow trout

To further determine the protective efficacy of the recombinant viruses against IHNV, the serum of rainbow trout was collected at 14, 28, 42, and 56 days post-infection after inoculation with the recombinant viruses. The antibody IgM levels were enhanced for a specific time in the groups rIHNV-$M_{(PH > A4)}$, rIHNV-$G_{(PS > A4)}$, rIHNV HLJ-09 and wtIHNV HLJ-09 but no increase was observed in antibody IgM levels in the control group after the challenge ($P < 0.01$), and there

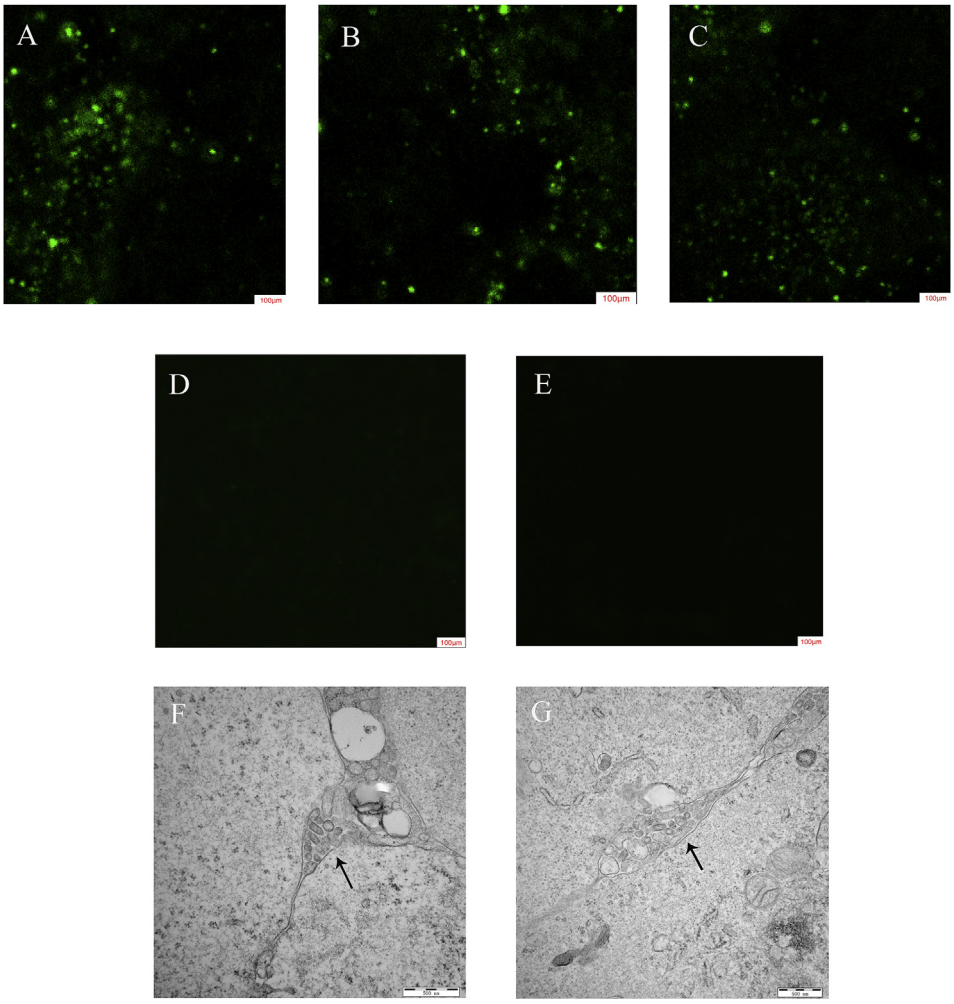

Fig. 3. Detection of the recombinant viruses by indirect immunofluorescence assay and transmission electron microscopy (TEM). After the CHSE-214 cells infected with rIHNV-$M_{(PH > A4)}$, rIHNV-$G_{(PS > A4)}$ or wtIHNV HLJ-09, mouse-anti-IHNV serum and fluorescein isothiocyanate (FITC)-conjugated goat anti-mouse immunoglobulin G (IgG) were respectively used as primary and secondary antibodies. The cells were observed under a microscope. (A) CHSE-cells infected with rIHNV-$M_{(PH > A4)}$. (B) CHSE-214 cells infected with rIHNV-$G_{(PS > A4)}$. (C) CHSE-214 cells infected with wtIHNV HLJ-09. (D) Normal CHSE-214 cells control. (E) Negative serum control. After inoculation with the recombinant viruses, the CHSE-214 cells were scraped off for TEM. The virions of rIHNV-$M_{(PH > A4)}$ were showed in F (scale bar 500 nm). The virions of rIHNV-$G_{(PS > A4)}$ were showed in G (scale bar 500 nm). Arrows indicated virions.

was no significant difference between the recombinant viruses (Fig. 8).

4. Discussion

Viral L domains are required for the efficient budding of many RNA-containing viruses [30]. The L domains include three motifs, PPXY, PT/SAP, or YxxL, which mediate interactions with host proteins to promote virus-cell separation [25,30]. This is consistent with our previous research showing that the ESCRT components in the host cells of fish that interact with the PPPH, PSAP or LXXLF motifs of IHNV proteins and this interaction recruits the ESCRT pathway to mediate viral budding [30,32]. Previous studies have shown that the PPPY-type L domain of the M protein of VSV (*Rhabdoviridae* family of viruses) plays a role in viral assembly and budding, host protein shut-off, and pathogenicity [19]. Additionally, the mutagenesis of the PSAP motif of VSV possesses a highly attenuated phenotype in mice, which showed that the viral PSAP motif affects viral pathogenicity [39]. Thus, to determine whether the L domains in the M and G proteins of IHNV have the role of

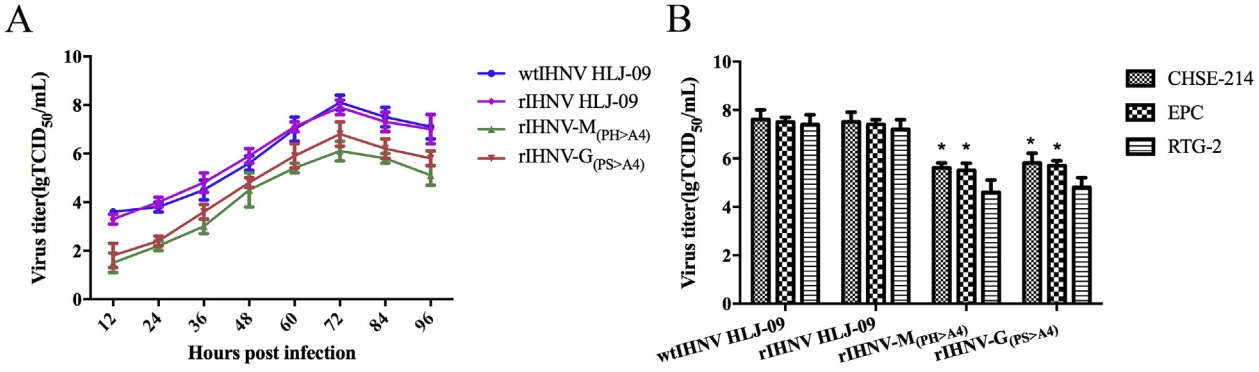

Fig. 4. Viral growth curves in CHSE-214 cells (A) and cell tropisms of wtIHNV HLJ-09, rIHNV HLJ-09 and recombinant viruses (B). (A) Cells were infected with rIHNV-$M_{(PH > A4)}$, rIHNV-$G_{(PS > A4)}$, rIHNV HLJ-09 or wtIHNV HLJ-09. The supernatants were harvested at 12 h intervals post-infection and titers were determined in CHSE-214 cells using the Reed-Muench method. (B) The recombinant viruses, rIHNV HLJ-09 or wtIHNV HLJ-09 were used to inoculate CHSE-214, EPC and RTG-2 cells. At 72 h post-infection the viral titers were determined (*$p < 0.05$ = .

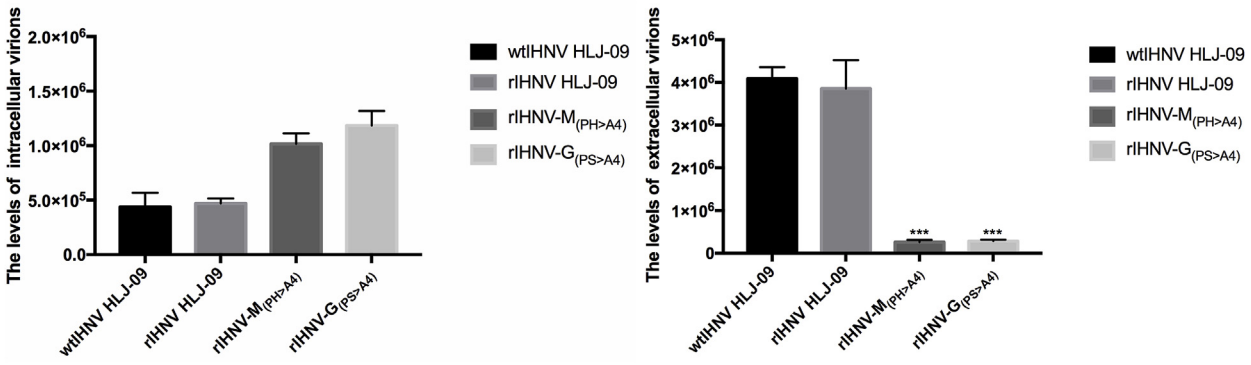

Fig. 5. Production of recombinant viruses. The CHSE-214 cells infected with rIHNV-$M_{(PH > A4)}$, rIHNV-$G_{(PS > A4)}$, rIHNV HLJ-09 or wtIHNV HLJ-09 for 72 h. In left, the cells were lysed to extract DNA for RT-qPCR using IHNV primers to quantify IHNV genomic concentration. In right, the supernatant of the cells was lysed to extract DNA, which were subjected to RT-qPCR using IHNV primers to quantify IHNV genomic concentration. Statistical analysis was performed using Student's t-test (***$p < 0.001$ = .

affecting the budding and possessing attenuated phenotype of the virus, we generated rIHNV-$M_{(PH > A4)}$ and rIHNV-$G_{(PS > A4)}$ in this study.

In this study, rIHNV-$M_{(PH > A4)}$ and rIHNV-$G_{(PS > A4)}$ were generated by reverse genetics and confirmed with RT-PCR, genetic tags, indirect IFA, and TEM analysis. Then, we found that the production levels of extracellular IHNV particles in cells infected with rIHNV-$M_{(PH > A4)}$ or rIHNV-$G_{(PS > A4)}$ declined significantly compared with those in cells infected with wtIHNV HLJ-09. The results demonstrated that the recombinant viruses reduced viral budding. A previous study showed that a series of recombinant RABVs, including mutations within the PPEY motif of the M protein, were generated by reverse genetics and their effects on viral replication and RABV pathogenicity were analyzed [28,40]. The authors suggested that the PPEY motif played a role in RABV release [40], which was consistent with our research. Also, RABV and IHNV belong to the *Rhabdoviridae* family of viruses. Therefore, these results illustrated that the L domains of *Rhabdoviridae* viruses could have a role in budding. Moreover, previous research showed that the double mutant in VSV is always much more affected than single mutant of VSV in whatever the cell lines were used, the yield of the infectious particle was systematically decreased by a factor of 5–10

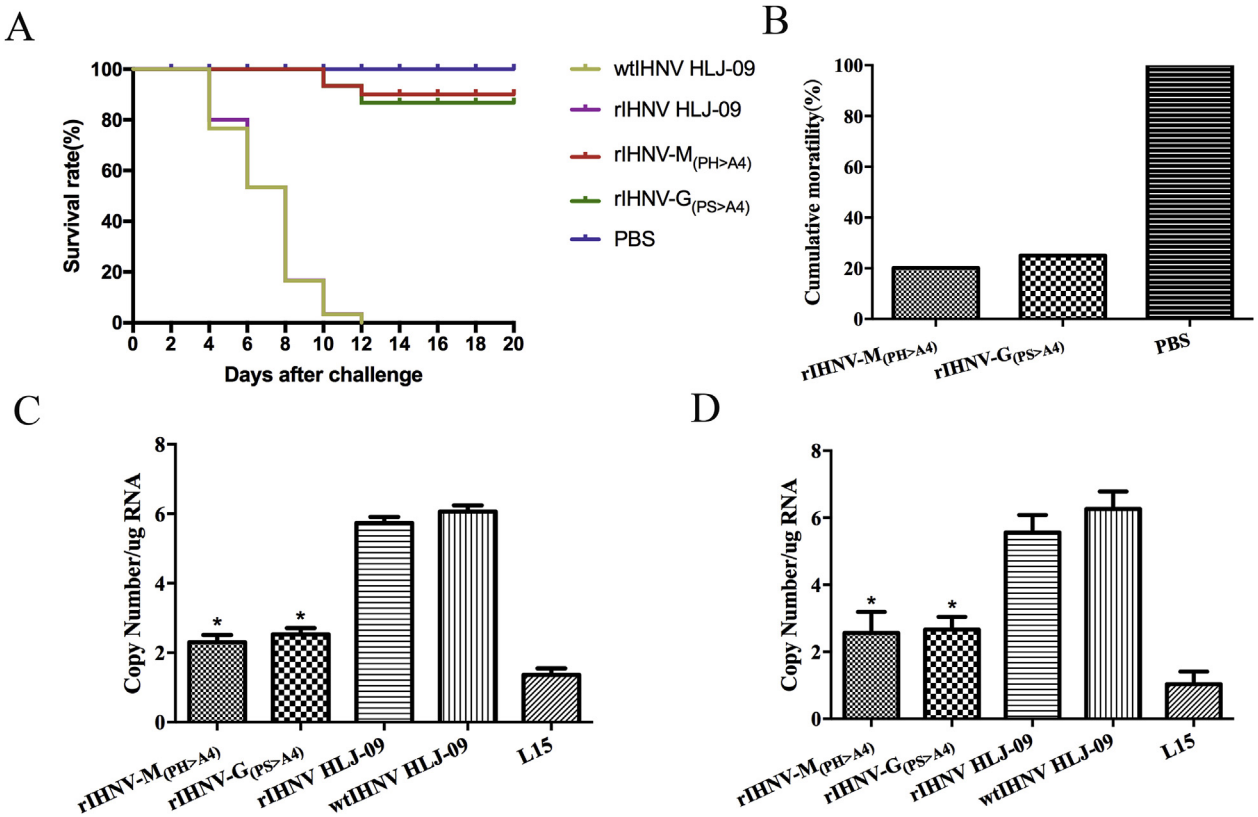

Fig. 6. Pathogenicity of recombinant viruses. (A) Survival rates of rainbow trout intraperitoneally injected with 50 μl (1×10^5 $TCID_{50}$/ml) of recombinant viruses and wtIHNV HLJ-09 were observed for 20 consecutive days. (B) Twenty-day cumulative mortality of fish vaccinated with rIHNV-$M_{(PH > A4)}$ or rIHNV-$G_{(PS > A4)}$ prior to challenge with wtIHNV HLJ-09. The number of survivors was recorded daily and data were analyzed using the GraphPad Prism v 5.0 software. The geometric mean of IHN viral load in liver (C) and kidney (D) measures at 72 h post-infection using RT-qPCR. The rainbow trout were infected with 200 μL (1×10^5 $TCID_{50}$/mL) of recombinant viruses, wtIHNV HLJ-09 and cell culture medium (L15) as the negative control. Single asterisks indicate significant decreases in viral load in two tissues of recombinant viruses at 72 h post-infection relative to wtIHNV HLJ-09 (*$p < 0.05$).

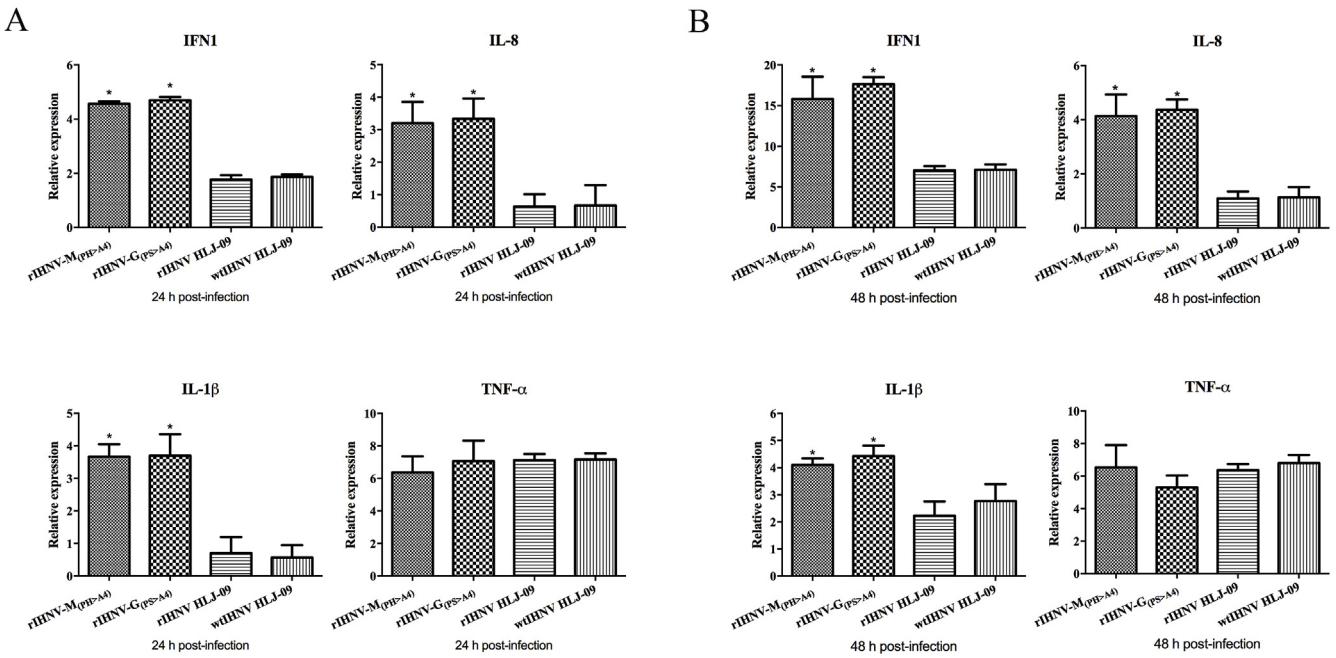

Fig. 7. Analysis of *IFN1, IL-8, IL-1β,* and *TNF-α* gene expression in rainbow trout using RT-qPCR. Fish were inoculated with rIHNV-$M_{(PH > A4)}$, rIHNV-$G_{(PS > A4)}$, rIHNV HLJ-09, wtIHNV HLJ-09 or volume-matched virus-free cell culture medium, and relative expression of *IFN1, IL-8, IL-1β,* and *TNF-α* gene in the spleen tissues were analyzed at 24 h (A) and 48 h pi (B) (*$p < 0.05$).

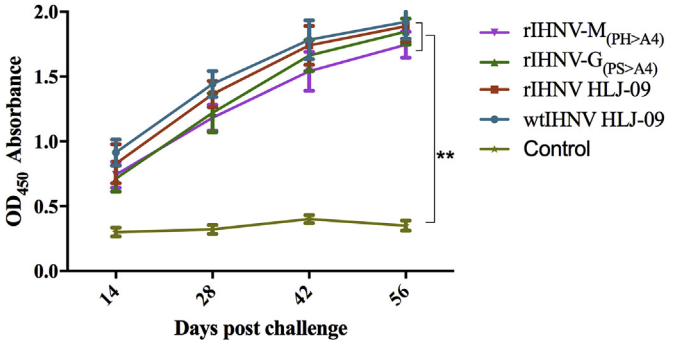

Fig. 8. Specific IgM antibody titers in vaccinated rainbow trout sera against the IHNV. After inoculation with the recombinant viruses and wtIHNV HLJ-09, the serum of rainbow trout was collected, and the levels of the specific IgM antibodies in the serum were measured by indirect ELISA. Data were analyzed using the GraphPad Prism v5.0 software. Asterisks indicate significant differences among the groups, as calculated by t tests analysis (**$p < 0.01$).

[41]. However, the idea that the double mutant of PPPH and PSAP in IHNV may affect much more strongly the budding of viruses than the single mutant remains to be determined. Additionally, we evaluated the pathogenicity of rIHNV-$M_{(PH > A4)}$ and rIHNV-$G_{(PS > A4)}$. The survival rates of juvenile rainbow trout infected with rIHNV-$M_{(PH > A4)}$ and rIHNV-$G_{(PS > A4)}$ were 90% and 87%, respectively. This result suggested that the recombinant viruses were highly attenuated, which was consistent with previous research showing that the mutant PSAP motif of VSV possesses a highly attenuated phenotype in mice [39]. Meanwhile, the survival rates of the rIHNV-$M_{(PH > A4)}$ and rIHNV-$G_{(PS > A4)}$ against wtIHNV HLJ-09 virus challenge were 80% and 75%, respectively. This showed that the two recombinant viruses have higher protective effects on rainbow trout. Also, the RT-qPCR analysis showed that the viral genome copy numbers in the liver and kidney of the fish infected with the recombinant viruses were lower than those in the liver and kidney of fish infected with wtIHNV HLJ-09 and rIHNV HLJ-09. These results suggested that the PPPH and PSAP motifs directly affected IHNV budding but indirectly affected viral replication and pathogenicity. Taken together, these findings strongly suggest that the PPPH and PSAP motifs possess L-domain activity in the context of IHNV infection and may be necessary for the pathogenic potential of the virus in an animal model.

We also studied the effect on the transcription of hallmark genes involved in the early immune response to rIHNV-$M_{(PH > A4)}$ or rIHNV-$G_{(PS > A4)}$. The RT-qPCR results showed that rIHNV-$M_{(PH > A4)}$ and rIHNV-$G_{(PS > A4)}$ could induce the expression of *IFN1, IL-1β*, and *IL-8* in the host, demonstrating that the two recombinant viruses could cause an adaptive immune response in the host and trigger the body's antiviral defenses [42]. Moreover, fish vaccinated with the recombinant viruses produced high levels of specific IgM antibodies, illustrating that the two recombinant viruses may induce immune responses in rainbow trout and resist infection by IHNV. These results indicated that the L domains were essential for both the efficient immune response and pathogenicity of IHNV.

In conclusion, we rescued the two recombinant viruses rIHNV-$M_{(PH > A4)}$ and rIHNV-$G_{(PS > A4)}$, while confirming the role of the L domains of the M and G proteins in IHNV budding and pathogenicity, which may provide beneficial insight into the viral pathogenesis of IHNV. Additionally, these results suggest that the attenuated vaccines have the potential application of being utilized as a viral vaccine. Also, these findings may be beneficial in the prevention and control of IHNV infections in fish.

Acknowledgements

This work was supported by the National Natural Science Foundation of China (Grant No.31672697; 31372568) and national natural fund international cooperation program (No.31511130137).

References

[1] A. Ammayappan, S.E. LaPatra, V.N. Vakharia, Molecular characterization of the virulent infectious hematopoietic necrosis virus (IHNV) strain 220-90, Virol. J. 7 (2010) 1–11.
[2] P. Dixon, R. Paley, R. Alegria-Moran, B. Oidtmann, Epidemiological characteristics of infectious hematopoietic necrosis virus (IHNV): a review, Vet. Res. 47 (2016) 1–26.
[3] P.J. Enzmann, G. Kurath, D. Fichtner, S.M. Bergmann, Infectious hematopoietic

necrosis virus: monophyletic origin of European isolates from North American genogroup M, Dis. Aquat. Org. 66 (2005) 187–195.
[4] S. Ahmadivand, M. Soltani, K. Mardani, S. Shokrpoor, R. Hassanzadeh, M. Ahmadpoor, H. Rahmati-Holasoo, S. Meshkini, Infectious hematopoietic necrosis virus (IHNV) outbreak in farmed rainbow trout in Iran: viral isolation, pathological findings, molecular confirmation, and genetic analysis, Virus Res. 229 (2017) 17–23.
[5] R.R. Rucker, W.J. Whipple, J.R. Parvin, C.A. Evans, A Contagious Disease of Salmon Possibly of Virus Origin vol. 76, Washington the Service Usgovt Printoff, 1953.
[6] M. Adel, A.B. Amiri, M. Dadar, R. Breyta, G. Kurath, B. Laktarashi B, et al., Phylogenetic relationships of Iranian infectious hematopoietic necrosis virus of rainbow trout (Oncorhynchus mykiss) based on the glycoprotein gene, Arch. Virol. 161 (2016) 657–663.
[7] M.K. Purcell, S.E. Lapatra, J.C. Woodson, G. Kurath, J.R. Winton, Early viral replication and induced or constitutive immunity in rainbow trout families with differential resistance to Infectious hematopoietic necrosis virus (IHNV), Fish Shellfish Immunol. 28 (2012) 98–105.
[8] L.R. Pierce, C.A. Stepien, Evolution and biogeography of an emerging quasis-species: diversity patterns of the fish Viral Hemorrhagic Septicemia virus (VHSV), Mol. Phylogenetics Evol. 63 (2012) 327–341.
[9] S.L. Rudakova, G. Kurath, E.V. Bochkova, Occurrence and genetic typing of infectious hematopoietic necrosis virus in Kamchatka, Russ. Dis. Aquat. Org. 75 (2007) 1–11.
[10] S.P. Morzunov, J.R. Winton, S.T. Nichol, The complete genome structure and phylogenetic relationship of infectious hematopoietic necrosis virus, Virus Res. 38 (1995) 175–192.
[11] R. Assenberg, O. Delmas, B. Morin, S.C. Graham, X.D. Lamballerie, et al., Genomics and structure function studies of Rhabdoviridae proteins involved in replication and transcription, Antivir. Res. 87 (2010) 149–161.
[12] M.S. Kim, K.H. Kim, Protection of olive flounder, Paralichthys olivaceus, against viral hemorrhagic septicemia virus (VHSV) by immunization with NV gene-knockout recombinant VHSV, Aquaculture 314 (2011) 39–43.
[13] P. Pereiro, A.M. Lopez, A. Falco, S. Dios, A. Figueras, J.M. Coll, B. Novoa, A. Estepa, Protection and antibody response induced by intramuscular DNA vaccine encoding for viral haemorrhagic septicaemia virus (VHSV) G glyco- protein in turbot (Scophthalmus maximus), Fish Shellfish Immunol. 32 (2012) 1088–1094.
[14] A. Ammayappan, V.N. Vakharia, Nonvirion protein of novirhabdovirus suppresses apoptosis at the early stage of virus infection, J. Virol. 85 (2011) 8393–8402.
[15] S. Biacchesi, M.I. Thoulouze, M. Bearzottim, Y.X. Yu, M. Bremont, Recovery of NV knockout infectious hematopoietic necrosis virus expressing foreign genes, J. Virol. 74 (2000) 11247–11253.
[16] S. Biacchesi, The reverse genetics applied to fish RNA viruses, Vet. Res. 42 (2011) 12–20.
[17] P.J. Walker, R.G. Dietzgen, D.A. Joubert, K.R. Blasdell, Rhabdovirus accessory genes, 162 (2011) 110–125.
[18] Y.P. Chen, M.T. Guo, Y.X. Wang, X.J. Hua, S. Gao, Y.T. Wang, D.C. Li, et al., Immunity induced by recombinant attenuated IHNV (infectious hematopoietic necrosis virus)-G^{N438A} expresses *VP2* gene encoded IPNV (infectious pancreatic necrosis virus) against both pathogens in rainbow trout, J. Fish Dis. 42 (2019) 631–642.
[19] E. Carnero, R.N. Harty, T. Irie, Adolfo GarcíaSastre, A. Okumura, Modifications of the psap region of the matrix protein lead to attenuation of vesicular stomatitis virus in vitro and in vivo, J. Gen. Virol. 88 (2007) 2559–2567.
[20] B. Dancho, M.O. Mckenzie, J.H. Connor, D.S. Lyles, Vesicular stomatitis virus matrix protein mutations that affect association with host membranes and viral nucleocapsids, J. Biol. Chem. 284 (2009) 4500–4509.
[21] A.A.V. Albertini, G. Schoehn, W. Weissenhorn, R.W.H. Ruigrok, Structural aspects of rabies virus replication, Cell. Mol. Life Sci. 65 (2008) 282–294.
[22] J. Votteler, W.I. Sundquist, Virus budding and the ESCRT pathway, Cell Host Microbe 14 (2013) 232–241.
[23] B.J. Chen, R.A. Lamb, Mechanisms for enveloped virus budding: can some viruses do without an ESCRT? Virology 372 (2008) 221–232.
[24] H.R. Jayakar, E. Jeetendra, M.A. Whitt, Rhabdovirus assembly and budding, Virus Res. 106 (2004) 117–132.
[25] E.O. Freed, Viral late domains, J. Virol. 76 (2002) 4679–4687.
[26] A. Pincetic, J. Leis, The mechanism of budding of retroviruses from cell membranes, Adv. Virol. 2009 (2009) 1–9.
[27] S.J. Martin, C.D. Perez, P.D. Bieniasz, Context-dependent effects of l domains and ubiquitination on viral budding, J. Virol. 78 (2004) 5554–5563.
[28] A. Okumura, R.N. Harty, Rabies virus assembly and budding, Adv. Virus Res. 79 (2011) 23–32.
[29] J. Yasuda, M. Nakao, Y. Kawaoka, H. Shida, Nedd4 regulates egress of ebola virus-like particles from host cells, J. Virol. 77 (2003) 9987–9992.
[30] T. Irie, R.N. Harty, L-domain flanking sequences are important for host interactions and efficient budding of vesicular stomatitis virus recombinants, J. Virol. 79 (2005) 12617–12622.
[31] L. VerPlank, F. Bouamr, T.J. LaGrassa, B. Agresta, A. Kikonyogo, J. Leis, et al., Tsg101, a homologue of ubiquitin-conjugating (E2) enzymes, binds the L domain in HIV type 1 Pr55(Gag), Proc. Natl. Acad. Sci. 98 (2001) 7724–7729.
[32] Y.P. Chen, J.H. Li, Y. Zhou, Y. Feng, X. Guan, D.C. Li, et al., The role of infectious hematopoietic necrosis virus (IHNV) proteins in recruiting the ESCRT pathway through three ways in the host cells of fish during IHNV budding, Fish Shellfish Immunol. 92 (2019) 833–841.
[33] C. Wang, G.H. Lian, L.L. Zhao, Y. Wu, Y.J. Li, L.J. Tang, et al., Virulence and serological studies of recombinant infectious hematopoietic necrosis virus (IHNV) in rainbow trout, Virus Res. 220 (2016) 193–202.
[34] M. Guo, W. Shi, Y. Wang, Y. Wang, Y. Chen, D. Li, et al., Recombinant infectious hematopoietic necrosis virus expressing infectious pancreatic necrosis virus vp2 protein induces immunity against both pathogens, Fish Shellfish Immunol. 78 (2018) 187–194.
[35] Y. Wu, L. Wang, T. Guo, Y. Jiang, X. Qiao, L. Sun, et al., Identification of amino acid residues in infectious hematopoietic necrosis virus (ihnv) nv protein necessary for viral replication and pathogenicity, Fish Shellfish Immunol. 79 (2018) 294–302.
[36] L.J. Reed, H. Muench, A simple method of estimating fifty per cent endpoints, Am. J. Hyg. 27 (1938).
[37] S. Jia, G. Ding, C. Wang, B. Feng, Z. Wang, L. Wang, et al., N-linked glycosylation sites in G protein of infectious hematopoietic necrosis virus (IHNV) affect its virulence and immunogenicity in rainbow trout, Fish Shellfish Immunol. 89 (2019) 537–547.
[38] K.J. Livak, T.D. Schmittgen, Analysis of relative gene expression data using real-time quantitative PCR and the $2^{-\Delta\Delta Ct}$ Method, Methods 25 (2001) 402–408.
[39] T. Irie, Y.L. Liu, B.S. Drolet, E. Carnero, A. García-Sastre, R.N. Harty, Cytopathogenesis of vesicular stomatitis virus is regulated by the PSAP motif of M protein in a species-dependent manner, Viruses 4 (2012) 1605–1618.
[40] C. Wirblich, G.S. Tan, A. Papaneri, P.J. Godlewski, J.M. Orenstein, R.N. Harty, et al., PPEY motif within the rabies virus (RV) matrix protein is essential for efficient virion release and RV pathogenicity, J. Virol. 82 (2008) 9730–9738.
[41] L. Obiang, H. Raux, M. Ouldali, D. Blondel, Y. Gaudin, Phenotypes of vesicular stomatitis virus mutants with mutations in the psap motif of the matrix protein, J. Gen. Virol. 93 (2012) 857–865.
[42] V. Bergan, S. Steinsvik, H. Xu, Ø. Kileng, B. Robertsen, Promoters of type i interferon genes from atlantic salmon contain two main regulatory regions, FEBS J. 273 (2010) 3893–3906.